Spatial Realization of Escher's Impossible World

Kokichi Sugihara

Abstract— **M. C. Escher, a Dutch artist, created a series of lithographs presenting "impossible" objects and "impossible" motions. Although they are usually called "impossible", some of them can be realized as solid objects and physical motions in the three-dimensional space. The basic idea for these realizations is to use the degrees of freedom in the reconstruction of solids from pictures. First, the set of all solids represented by a given picture is represented by a system of linear equations and inequalities. Next the distribution of the freedom is characterized by a matroid extracted from this system. Then, a robust method for reconstructing solids is constructed and applied to the spatial realization of the "impossible" world.**

I. Introduction

There is a class of pictures called "anomalous pictures" or "pictures of impossible objects". These pictures generate optical illusion; when we see them, we have impressions of three-dimensional object structures, but at the same time we feel that such objects are not realizable. The Penrose triangle [13] is one of the oldest such pictures. Since the discovery of this triangle, many pictures belonging to this class have been discovered and studied in the field of visual psychology [9], [14].

The pictures of impossible objects have also been studied from a mathematical point of view. One of the pioneers is Huffman, who characterized impossible objects from a viewpoint of computer interpretation of line drawings [10]. Clowes [2] also proposed a similar idea in a different manner. Cowan [3], [4] and Térouanne [20] characterized a class of impossible objects that are topologically equivalent to a torus. Draper studied pictures of impossible object through the gradient space [6]. Sugihara classified pictures of impossible objects according to his algorithm for interpretation of line drawings [15], [16].

Impossible objects have also been used as material for artistic work by many artists. One of the most famous examples is the endless loop of stairs drawn by Dutch artist M. C. Escher in his work titled "Klimmen en dalen (Ascending and descending)" [8]. Other examples include painting by Mitsumasa Anno [1] and drawings by Sandro del Prete [7], to mention a few.

Those activities are stories about two-dimensional pictures. On the other hand, several tricks have also been found for realization of impossible objects as actual three-dimensional structures. The first trick is to use curved surfaces for faces that look planar; Mathieu Hamaekers generated the Penrose triangle by this trick [7]. The second trick is to generate hidden gaps in depth; Shigeo Fukuda used this trick and generated a solid model of Escher's "Waterfall" [7].

In this paper, we point out that some "impossible" objects can be realized as three-dimensional solids even if those tricks are not employed; in other words, "impossible" objects can be realized under the conditions that faces are made by planar (non-curved) polygons and that object parts are actually connected whenever they look connected in the picture plane. For example, Escher's endless loop of stairs can be realized as a solid model, as shown in Fig. 1 [17], [18]. We call this trick the "non-rectangularity trick", because those solid objects have non-rectangular face angles that look rectangular.

K. Sugihara is with the University of Tokyo, Tokyo 113-8656, Japan.

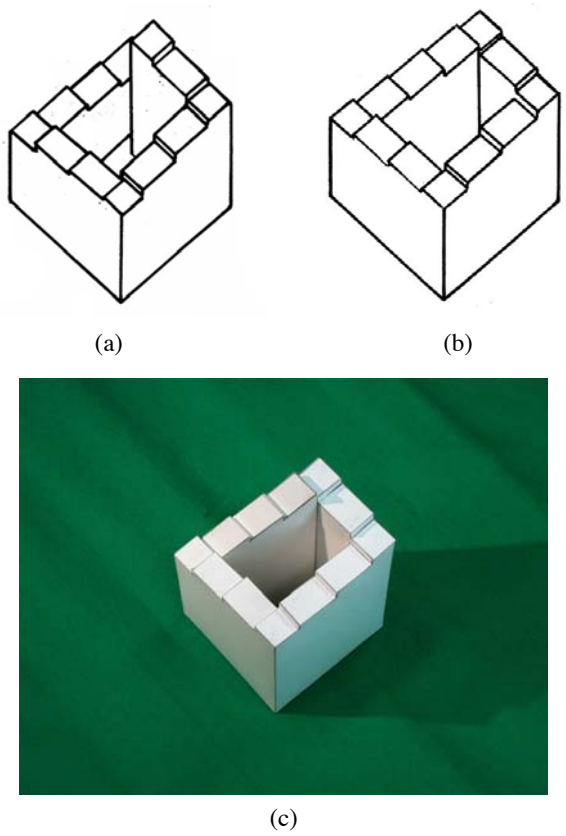

Fig. 1. Three-dimensional realization of Escher's endless loop of stairs: (a) ordinary picture; (b) picture of an impossible object; (c) solid model realized from the picture in (b).

The resulting solid models can generate optical illusions in the sense that although we are looking at actual objects, we feel that those objects can not exist. In all of those three tricks, we need to see the objects from a unique special point of view. Hence the illusion disappears if we move our eye positions. However, the non-rectangularity trick is less sensitive to the eye position, because the objects are made in such a way that faces that look planar are actually planar, and the parts that look connected are actually connected.

The non-rectangularity trick can also be used to generate a new class of visual illusion called "impossible" physical motions. The basic idea is as follows. Instead of pictures of impossible objects, we choose pictures of ordinary objects around us, and reconstruct solid models from these pictures using the non-rectangularity trick. The resulting solid models are unusual in their shapes although they look ordinary. Because of this gap between the perceived shape and the actual shape, we can add actual physical

motions that look like impossible.

The artist closest to the present work is M. C. Escher. Actually, he created many beautiful and interesting lithographs with mathematical flavor. Among many others, his works contain two groups; one is related to periodic tilings and the other is related to pictures of impossible objects. The former group, works based on periodic tilings, has been studied from a computational point of view by many scientists [5]; Recently, in particular, Kaplan and Salesin constructed a method called "Escherization" for designing Escher-like pictures based on tilings [11], [12].

From the viewpoint of computer-aided approach to Escher, the present paper is an attack on the other group, impossible objects and impossible motions. Actually, we represent a method for constructing three-dimensional solid objects and physical motions represented in Escher's lithographs. In this sense, what we are describing in this paper might be called "Three-Dimensionalization of the Escher World".

The organization of the paper is as follows. In Section II, we review the basic method for judging the realizability of a solid from a given picture, and in Section III, we review the robust method for reconstructing objects from pictures. In Section IV, we study how the degrees of freedom for reconstructing the solids are distributed in the picture. We show examples of the three dimensional realization of impossible objects and impossible motions in Section V and give conclusions in Section VI.

II. Freedom in the Back-Projection

In this section we briefly review the algebraic structure of the freedom in the choice of the polyhedron represented by a picture [16]. This gives the basic tool with which we construct our algorithm for designing impossible motions.

As shown in Fig. 2, suppose that an (x, y, z) Cartesian coordinate system is fixed in the three-dimensional space, and a given polyhedral object P is projected by the central projection with respect to the center at the origin $\mathrm{O} = (0, 0, 0)$ onto the picture plane $z = 1$. Let the resulting picture be denoted by D. If the polyhedron P is given, the associated picture D is uniquely determined. On the other hand, if the picture D is given, the associated polyhedron is not unique; there is large freedom in the choice of the polyhedron whose projection coincides with D. The algebraic structure of the degree of freedom can be formulated in the following way.

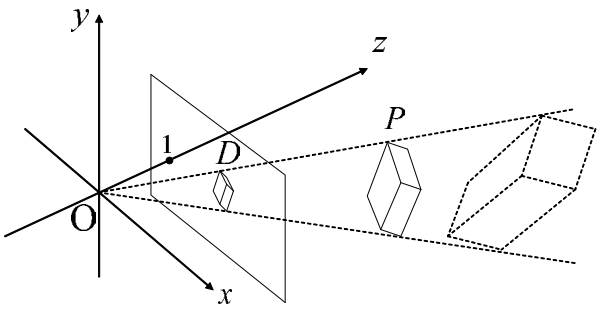

Fig. 2. Solid and its central projection.

For a given polyhedron P, let $V = \{v_1, v_2, \ldots, v_m\}$ be the set of all the vertices of P, $F = \{f_1, f_2, \ldots, f_n\}$ be the set of all the faces of P, and R be the set of all pairs (v_i, f_j) of vertices v_i $(\in V)$ and faces f_j $(\in F)$ such that v_i is on f_j. We call the triple $I = (V, F, R)$ the *incidence structure* of P.

Let (x_i, y_i, z_i) be the coordinates of the vertex v_i $(\in V)$, and let

$$a_j x + b_j y + c_j z + 1 = 0 \tag{1}$$

be the equation of the plane containing the face f_j $(\in F)$. The central projection $v_i' = (x_i', y_i', z_i')$ of the vertex v_i onto the picture plane $z = 1$ is given by

$$x_i' = x_i/z_i, \quad y_i' = y_i/z_i, \quad z_i' = 1. \tag{2}$$

Suppose that we are given the picture D and the incidence structure $I = (V, F, R)$, but we do not know the exact shape of P. Then, the coordinates of the projected vertices x_i' and y_i' are given constants, while z_i $(i = 1, 2, \ldots, m)$ and a_j, b_j, c_j $(j = 1, 2, \ldots, n)$ are unknown variables. Let us define

$$t_i = 1/z_i. \tag{3}$$

Then, we get

$$x_i = x_i'/t_i, \quad y_i = y_i'/t_i, \quad z_i = 1/t_i. \tag{4}$$

Assume that $(v_i, f_j) \in R$. Then, the vertex v_i is on the face f_j, and hence

$$a_j x_i + b_j y_i + c_j z_i + 1 = 0 \tag{5}$$

should be satisfied. Substituting (4), we get

$$x_i' a_j + y_i' b_j + c_j + t_i = 0, \tag{6}$$

which is linear in the unknowns a_j, b_j, c_j and t_i because x_i' and y_i' are known constants.

Collecting the equations of the form (6) for all $(v_i, f_j) \in R$, we get the system of linear equations, which we denote by

$$A\boldsymbol{w} = 0, \tag{7}$$

where $\boldsymbol{w} = (t_1, \ldots, t_m, a_1, b_1, c_1, \ldots, a_n, b_n, c_n)$ is the vector of unknown variables and A is a constant matrix.

The picture D also gives us information about the relative depth between a vertex and a face. Suppose that a visible face f_j hides a vertex v_i. Then, f_j is nearer to the origin than v_i, and hence we get

$$x_i' a_j + y_i' b_j + c_j + t_i < 0. \tag{8}$$

If the vector v_i is nearer than the face f_j, then we get

$$x_i' a_j + y_i' b_j + c_j + t_i > 0. \tag{9}$$

Collecting all of such inequalities, we get a system of linear inequalities, which we denote by

$$B\boldsymbol{w} > 0, \tag{10}$$

where B is a constant matrix.

The linear constraints (7) and (10) specify the set of all possible polyhedron represented by the given picture D. In other words, the set of all $\boldsymbol{w}$'s that satisfy the equations (7) and the inequalities (10) represents the set of all possible polyhedrons represented by D. Actually the next theorem holds.

Theorem 1. [16]. Picture D represents a polyhedron if and only if the system of linear equations (7) and inequalities (10) has a solution.

Hence, to reconstruct a polyhedron from a given picture D is equivalent to choose a vector $\boldsymbol{w}$ that satisfies (7) and (10). (Refer to [16] for the formal procedure for collecting the equation (7) and the inequalities (10) and for the proof of this theorems.)

III. Robust Reconstruction of Objects

As seen in the last section, we can characterize the set of all polyhedra represented by a given picture in terms of linear constraints. However, these constraints are too strict if we want to apply them to actual reconstruction procedure. This can be understood by the next example.

Consider the picture shown in Figure 3(a). We, human beings, can easily interpret this picture as a truncated pyramid seen from above. However, if we search by a computer for the vectors w that satisfy the constraints (7) and (10), the computer usually judges that the constraints (7) and (10) are not satisfiable and hence the picture in Figure 3(a) does not represent any polyhedron.

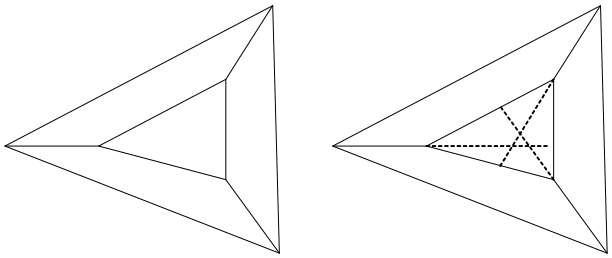

(a) (b)

Fig. 3. Picture of a truncated pyramid: (a) a picture which we can easily interpret as a truncated pyramid; (b) incorrectness of the picture due to lack of the common point of intersection of the three side edges that should be the apex of the pyramid.

This judgment is mathematically correct because of the following reason.

Suppose that Figure 3(a) represents a truncated pyramid. Then, its three side faces should have a common point of intersection at the apex of the pyramid when they are extended. Since this apex is also on the common edge of two side faces, it is also the common point of intersection of the three side edges of the truncated pyramid. However, as shown by the broken lines in Figure 3(b), the three side edges does not meet at a corner point. Therefore, this picture is not a projection of any truncated pyramid. The truncated pyramid can be reconstructed only when we use curved faces instead of planar faces.

By this example, we can understand that the satisfiability of the constraints (7) and (10) is not a practical solution of the problem of judging the reconstructability of polyhedra from a picture. Indeed, digitization errors cannot be avoided when the pictures are represented in a computer, and hence the picture of a truncated pyramid becomes almost always incorrect even if we carefully draw it in such a way that the three side edges meet at a common point.

This kind of superstrictness of the constraints comes from redundancy of the set of linear equations. Actually, if the vertices of the truncated pyramid were placed at strictly correct positions in the picture plane, the associated coefficient matrix A is not of full rank. If those vertices contain digitization errors, the rank of the matrix A increases and consequently the set of constraints (7) and (10) becomes infeasible.

So in order to make a robust method for judging the reconstructability of polyhedra, we have to remove redundant equations from (10). For this purpose, the next theorem is helpful. Suppose that we are given a picture with the incidence structure $I = (V, F, R)$. For subset $X \subset F$, let us define

$$V(X) \equiv \{v \in V \mid (\{v\} \times F) \cap R \neq \emptyset\}, \tag{11}$$

$$R(X) \equiv (V \times X) \cap R, \tag{12}$$

that is, $V(X)$ $(\subset V)$ denotes the set of vertices that are on at least one face in X, and $R(X)$ $(\subset R)$ denotes the set of incidence pairs (v, f) such that $f \in X$. For any finite set X, let $|X|$ denote the number of elements in X. Then the next theorem holds.

Theorem 2 [16]. The associated set of equations (10) is nonredundant if and only if

$$|V(X)| + 3|X| \geq |R(X)| + 4 \tag{13}$$

for any subset $X \subset F$ such that $|X| \geq 2$.

Refer to [Sugihara 1986] for the strict meaning of "nonredundant" and for the proof.

For example, the picture in Figure 3(a) has 6 vertices and five faces (including the rear face) and hence $|V|+3|F| = 21$. On the other hand, this picture has 2 triangular faces and 3 quadrilateral faces, and hence has $|R| = 2 \times 3 + 3 \times 4 = 18$ incidence pairs in total. Therefore, the inequality (13) is not satisfied and consequently we can judge that the associated equations are redundant. Theorem 2 also tells us that if we remove any one equation from (10), the resulting equation becomes nonredundant.

In this way, we can use this theorem to judge whether the given incidence structure generates redundant equations, and also to remove redundancy if redundant.

Using Theorems 1 and 2, we can design a robust method for reconstructing a polyhedron from a given picture in the following way.

Suppose that we are given a picture. We first construct the equations (7) and the inequalities (10). Next, using Theorem 2, we judge whether (7) is redundant, and if redundant, we remove equations one by one until they become nonredundant. Let the resulting equations be denoted by

$$A'w = 0, \tag{14}$$

where A' is a submatrix of A obtained by removing the rows corresponding to redundant equations. Finally, we judge whether the system of (10) and (14) has solutions. If it has, we can reconstruct the solid model corresponding to an arbitrary one of the solutions. If it does not, we judge that the picture does not represent any polyhedron.

With the help of this procedure, Sugihara found that actual solid models can be reconstructed from some of pictures of impossible objects [17], [18].

IV. Distribution of the Degrees of Freedom

Let us concentrate on the solutions of eq. (7). This system of equations contains $m+3n$ unknown variables, whereas the number of essentially different equations is represented by $\mathrm{rank}(A)$. Hence, the degrees of freedom in the choice of eq. (7) can be represented by

$$m + 3n - \mathrm{rank}(A). \tag{15}$$

This number can also be interpreted as the degrees of freedom in the choice of the solid from the picture, because different solutions of eq. (7) correspond to different solids represented by the picture. Now, we are interested in how the degrees of freedom

are distributed; in other words, we want to know how freely we can deform each part of the solid from an ordinary shape.

We rewrite the vector $\boldsymbol{w} = (t_1, \ldots, t_m, a_1, b_1, c_1, \ldots, a_n, b_n, c_n)$ of unknowns as $\boldsymbol{w} = (u_1, u_2, \ldots, u_{m+3n})$. Let H denote the set of all unknowns, that is, $H = \{t_1, \ldots, t_m, a_1, b_1, c_1, \ldots, a_n, b_n, c_n\} = \{u_1, u_2, \ldots, u_{m+3n}\}$. For each $u_i \in H$, let $\boldsymbol{e}_i$ be the $(m + 3n)$-dimensional row vector whose ith component is 1 and all the other components are 0's. Then, for a real number d_i, the equation

$$\boldsymbol{e}_i \cdot \boldsymbol{w} = d_i$$

represents the constraints that the value of the unknown u_i is fixed to d_i.

For any subset $X \subset H$, let $A \cup \{\boldsymbol{e}_i \mid u_i \in X\}$ denote the matrix obtained by adding the row vectors in $\{\boldsymbol{e}_i \mid u_i \in X\}$ to the matrix A, and we define $\rho(X)$ as

$$\rho(X) \equiv \mathrm{rank}(A \cup \{\boldsymbol{e}_i \mid u_i \in X\}) - \mathrm{rank}(A). \qquad (16)$$

$\rho(X)$ represents the maximum number of unknowns in X whose values can be fixed arbitrarily and still can construct the solution of eq. (7). Hence, the value $\rho(X)$ can be interpreted as the degrees of freedom of the subset X of the unknowns.

From the definition, ρ is a rank function of a matroid; indeed (H, ρ) is the matroid obtained from the linear matroid consisting of all the row vectors in the matrix $A \cup \{\boldsymbol{e}_i \mid u_i \in H\}$ by the contraction with respect to the row vectors in A [21]. This matroid characterizes the distribution of the degrees of freedom in the choice of a solid represented by a given picture. Hence, this matroid gives us information about how freely we can deform a solid from its natural shape so that we can add physical motions that look impossible [19], as we will see by examples in the next section.

V. Examples

The first examples of the realization of the impossible object shown in Fig. 1(c) was constructed in the following manner. First, we construct the system of equations (7) for the picture in Fig. 1(b), then, removed redundant equations using Theorem 2 and got a non-redundant system (14) of equations. Next, we got a solution of eq. (14), which represents a specific shape of the three-dimensional solid. Finally, we computed the figure of an unfolded surfaces of this solid, and made the paper model by hands.

Fig. 4 shows another view of this solid. As we can understand from this figure, some of the steps of the endless stair are not horizontal, which makes it possible to connected the steps into an endless loop.

Fig. 5(a) shows another example of an impossible object constructed in a similar manner. In this object, the near-far relations of the poles seem inconsistent; some poles are nearer than others on the floor while they are farther at the ceiling. This inconsistent structure is essentially similar to that represented by Escher's lithograph "Belvédère" in 1958. Fig. 5(b) shows the same solid seen from a different direction.

Next, let us consider "impossible" physical motions. A typical example of impossible motions is represented in Escher's lithograph "Waterval" in 1961, in which water is running uphill through the water path and is falling down at the waterfall, and is running uphill again. This motion is really impossible because

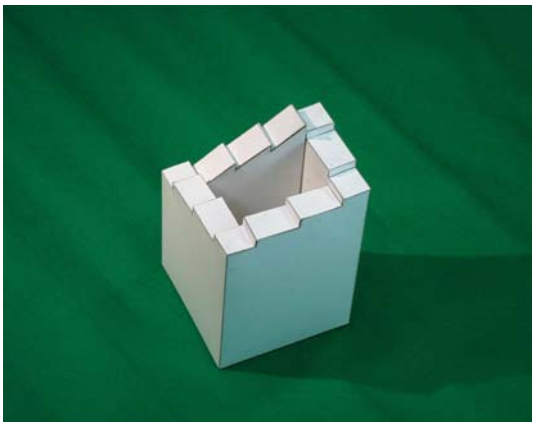

Fig. 4. Endless loop of stairs shown in Fig. 1(c) seen from a different viewpoint.

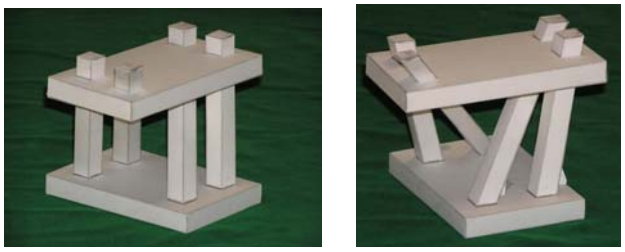

(a) (b)

Fig. 5. "Impossible" columns: (a) shows an impossible structure which is similar to Escher's lithograph "Belvédère"; (b) shows another view of the same solid.

otherwise an eternal engine could be obtained but that contradicts the physical law.

However, this impossible motion is realizable partially in the sense that material looks running uphill a slope. An example of this impossible motion is shown in Fig. 6. Fig. 6(a) shows a solid consisting of three slopes, all of which go down from the right to the left. If we put a ball on the left edge of the leftmost slope, as shown in Fig. 6(a), the ball moves climbing up the three slopes from the left to the right one by one; thus the ball admits an impossible motion.

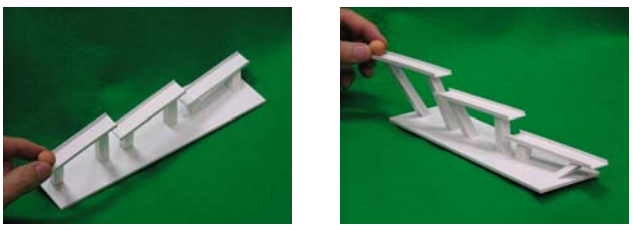

(a) (b)

Fig. 6. Impossible motion of a ball along "Antigravity Three Slopes": (a) a ball climbing up the slopes; (b) another view of the same situation.

The actual shape of this solid can be understood if we see Fig. 6(b), which is the photograph of the same solid as in Fig. 6(a) seen from another direction. From this figure, we can see that actually the ball is just rolling down the slopes according to the natural properties of the ball and the slopes.

Still another example is shown in Figure 7. In this figure, there are two windows that look connected in a usual manner but a

straight bar passes through them in an unusual way.

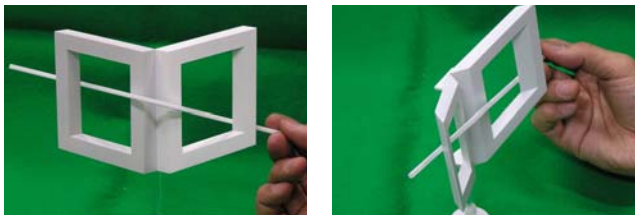

(a) (b)

Fig. 7. "Distorted Windows": (a) a straight bar passing throw the two windows in an unusual manner; (b) another view.

VI. Concluding Remarks

We have presented a method for creating "impossible" objects and "impossible" motions. In this method, the design of a solid admitting impossible objects and motions is formulated as a search for feasible solutions of a system of linear equations and inequalities. The resulting method enables us to realize Escher's impossible world in the three-dimensional space.

The impossible objects and motions obtained by this method can offer a new type of optical illusion. When we see these objects and motions, we have a strange impression in the sense that we feel they are impossible although we are actually seeing them. Hence it is one of our future work to study this type of optical illusion from a view point of visual psychology.

Other future problems include (1) collecting other variants of impossible objects and motions created by the present method, and (2) formulating the objective functions for selecting optimal shapes among all the solids specified by the distribution of the degrees of freedom.

References

[1] M. Anno, *Book of ABC* (in Japanese), Fukuinkan-Shoten, Tokyo, 1974.
[2] M. B. Clowes, "On seeing things," *Artificial Intelligence*, vol. 2, pp. 79–116, 1971.
[3] T. M. Cowan, "The theory of braids and the analysis of impossible figures," *Journal of Mathematical Psychology*, vol. 11, pp. 190–212, 1974.
[4] T. M. Cowan, "Organizing the properties of impossible figures," *Perception*, vol. 6, pp. 41–56, 1977.
[5] H. S. M. Coxeter, M. Emmer, R. Penrose and M. L. Teuber, *M. C. Escher — Art and Science*, North-Holland, Amsterdam, 1986.
[6] S. W. Draper, "The Penrose triangle and a family of related figures," *Perception*, vol. 7, pp. 283–296, 1978.
[7] B. Ernst, *The Eye Beguiled*, Benedict Taschen Verlag GmbH, Köln, 1992.
[8] M. C. Escher, *Evergreen*, Benedict Taschen Verlag GmbH, Köln", 1993.
[9] R. L. Gregory, *The Intelligent Eye*, third edition, Weiderfeld and Nicolson, London, 1971.
[10] D. A. Huffman, "Impossible objects as nonsense sentences," In *Machine Entelligence*, B. Metzer and D. Michie (eds.), vol. 6, Edinburgh University Press, 1971.
[11] C. S. Kaplan and D. H. Salesin, "Escherization," *Proceedings of ACM SIGGRAPH 2000*, ACM Press, New York, pp. 499–510, 2000.
[12] C. S. Kaplan and D. H. Salesin, "Dihedral Escherization," *Proceedings of Graphics Interface 2004*, pp. 255–262, 2004.
[13] L. S. Penrose and R. Penrose, "Impossible objects — A special type of visual illusion," *British Journal of Psychology*, vol. 49, pp. 31–33, 1958.
[14] J. O. Robinson, *The Psychology of Visual Illusion*, Hutchinson, London, 1972.
[15] K. Sugihara, "Classification of impossible objects," *Perception*, vol. 11, pp. 65–74, 1982.
[16] K. Sugihara, *Machine Interpretation of Line Drawings*, MIT Press, Cambridge, 1986.
[17] K. Sugihara, *Joy of Impossible Objects* (in Japanese), Iwanami-Shoten, Tokyo, 1997.
[18] K. Sugihara, "Three-dimensional realization of anomalous pictures—An application of picture interpretation theory to toy design," *Pattern Recognition*, vol. 30, no. 9, pp. 1061–1067, 1997.
[19] K. Sugihara, "A characterization of a class of anomalous solids," *Interdisciplinary Information Science*, vol. 11, pp. 149–156, 2005.
[20] E. Térouanne, "On a class of 'Impossible' figures: A new language for a new analysis," *Journal of Mathematical Psychology*, vol. 22, pp. 20–47, 1980.
[21] D. J. A. Welsh, *Matroid Theory*, Academic Press, London, 1976.

Kokichi Sugihara Kokichi Sugihara received the B. Eng., M. Eng. and Dr. Eng. in 1971, 1973 and 1980 respectively, from the University of Tokyo. He worked at Electrotechnical Laboratories of the Japanese Ministry of International Trade and Industry, and Nagoya University. He is now a professor of the Department of Mathematical Informatics of the University of Tokyo. His research interests include computational geometry, robust geometric computation, computer vision and computer graphics. He is the author of "Machine Interpotation of Line Drawings" (MIT Press, 1986), and a coauthor of "Spatial Tessellations—Concepts and Applications of Voronoi Diagrams" (John Wiley, 1992, 2000). He is a member of Japan SIAM, Operations Research Society of Japan, ACM, IEEE, etc.

This is a reproduction with permission of the paper originally published in the Proceedings of 8th Hellenic-European Conference on Computer Mathematics and Its Applications (HERCMA 2007), Athen, Greece, September 20-22, 2007, edited by Elias A. Lipitakis.

Kokichi Sugihara is currently Specially Appointed Professor in Meiji Institute for Advanced Study of Mathematical Sciences, Organization for the Strategic Coordination of Research and Intellectual Property, Meiji University.

Many interesting materials can be accessed at
http://home.mims.meiji.ac.jp/~sugihara/Welcome
including Professor Sugihara's prize winning project "Impossible Motion: Magnet-like Slopes" which won the 2010 Best Illusion of the Year Contest (see figure below).